

# Synthesis, Thermal and Spectroscopic Characterization of Caq<sub>2</sub> (Calcium 8-Hydroxyquinoline) Organic Phosphor

I. M. Nagpure · M. M. Duvenhage · Shreyas S. Pitale ·  
O. M. Ntwaeaborwa · J. J. Terblans · H. C. Swart

Received: 25 August 2011 / Accepted: 29 May 2012 / Published online: 9 June 2012  
© Springer Science+Business Media, LLC 2012

**Abstract** Bluish-green photoluminescence from calcium 8-hydroxyquinolate (Caq<sub>2</sub>) powder, synthesized by a co-precipitation route, and a blended Caq<sub>2</sub>:PMMA thin film is reported. The film was obtained by mixing the Caq<sub>2</sub> powder with PMMA (Polymethylmethacrylate) in a chloroform solution. X-ray diffraction analyses confirm the formation of the Caq<sub>2</sub> powder and thin film. Further structural elucidation was carried out using Fourier transform infrared spectroscopy (FTIR) in which the stretching frequencies of the Caq<sub>2</sub> bonds were determined. Bluish-green photoluminescence with a maximum at 480 nm was observed from the powder and the emission was red-shift by 10 nm in the case of the thin film. The UV-vis absorption bands were split and shifted due to different orientations of the Caq<sub>2</sub> molecules in both the powder and thin film. It was confirmed by thermogravimetric (TGA) and differential thermal analysis (DTA) that the Caq<sub>2</sub> powder was stable up to  $\approx 380$  °C. Atomic force microscopy images showed the continuous distribution of the Caq<sub>2</sub> atoms in the PMMA thin film. X-ray photoelectron spectroscopy data was used to estimate the binding energies of the chemical bonding in the Caq<sub>2</sub> powder complex. The optical properties of the Caq<sub>2</sub> powder and thin film were evaluated for possible application in organic light emitting devices.

**Keywords** Caq<sub>2</sub> · PL · XRD · FTIR · AFM · OLED

I. M. Nagpure · M. M. Duvenhage · S. S. Pitale ·  
O. M. Ntwaeaborwa · J. J. Terblans · H. C. Swart (✉)  
Department of Physics, University of the Free State,  
P. O. Box 339, Bloemfontein 9300, Republic of South Africa  
e-mail: swarthc@ufs.ac.za

I. M. Nagpure  
e-mail: indrajitnagpure@gmail.com

## Introduction

In recent years, research focus has been on the synthesis and characterization of light-emitting organic compounds for possible application in different types of electroluminescent devices [1, 2]. In most cases, the focus has mainly been on the electronic and geometric structures of polymer compounds that contains quinolate groups such as tris(8-hydroxyquinoline) aluminium (III) or Alq<sub>3</sub> and bis(8-hydroxyquinoline) zinc (II) or Znq<sub>2</sub> [3, 4]. Although many other different materials are used in electroluminescence devices for different purposes, Alq<sub>3</sub> still remains the material of choice for most basic and applied research [5]. For example, Alq<sub>3</sub> is widely used in organic light emitting diodes (OLEDs) as electron transporting and green emitting layer. Emission inefficiency and shorter life time [6] are, however, still major challenges facing Alq<sub>3</sub> in many technological and industrial applications [2, 3, 6]. Although it has been reported that Znq<sub>2</sub> has advantages such as higher injection efficiency, low operating voltage and high quantum yields compared to Alq<sub>3</sub> [7, 8], it has also been reported to be insoluble in common solvent making it difficult to study its luminescent properties in solvated media [1]. One other complex polymer that can be used in OLEDs is bis(8-hydroxyquinoline) Ca (II) or Caq<sub>2</sub> because of its resemblance to Znq<sub>2</sub>. In addition, Caq<sub>2</sub> has advantage such as comparable absolute photoluminescence efficiency to Alq<sub>3</sub> and Znq<sub>2</sub> [9]. However, limited basic information on the structure and optical properties, among other things, of this compound in the literature could be one of the reasons why it is less popular than Alq<sub>3</sub> and Znq<sub>2</sub>. As a result, this study sets out to evaluate the crystal structure, optical and thermal properties of Caq<sub>2</sub> in powder and polymethylmethacrylate

(PMMA) blended thin film forms. The structure, optical properties and thermal stability of the power and thin  $\text{Caq}_2$  film samples were analyzed using X-ray diffraction (XRD) and Fourier transform infrared spectroscopy (FTIR), Uv-vis absorption and fluorescence spectroscopies and the thermal stability was analyzed using Differential Thermal Analysis and Thermal Gravimetry Analysis (DTG-TG) respectively. In addition, the chemical and electronic states of the samples were analyzed using X-ray photoelectron spectroscopy while the surface topography was analyzed by atomic force microscopy.

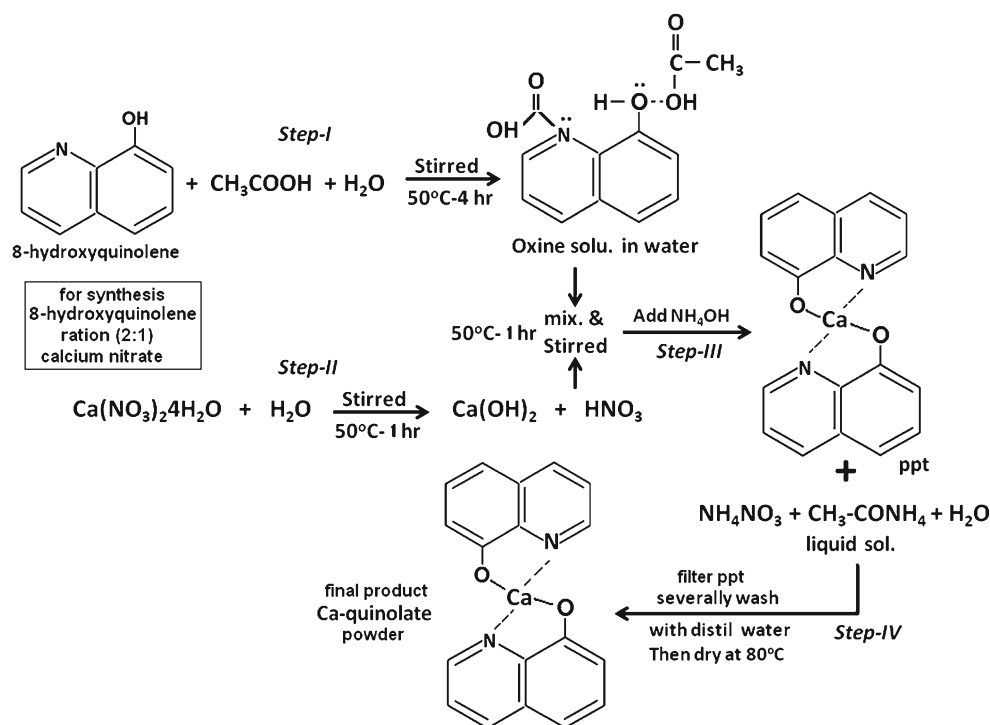
As widely reported in the literature, the nature of an attached metal ion influences the emission color, efficiency, stability and evaporability of metal quinoline derivatives. For example, changing the central metal ions (like Al, Ga, Zn) was shown to influence the photoluminescence peak position of the metal quinoline derivatives [9, 10]. In addition, its fluorescence efficiency has been shown to decrease with increasing atomic number of the metal ion, which is caused by an increase in intersystem crossing known as heavy atom effect [10]. For example, green emission is observed when a quinolate complex is doped with the Zn metal ion, and when the Zn ion is substituted by the Ca ion, the emission is blue-shifted. If calcium complexes are typically coordinated by organic ligands that provide the effectiveness of the sensitization and a subsequent enhancement of the luminescence intensity [9], they can then be used as potential optical emitters in OLED devices and amplifiers.

## Experimental

### Synthesis Method

The co-precipitation method was used to synthesize crystalline  $\text{Caq}_2$  (calcium hydroxyquinoline). Calcium nitrate ( $\text{Ca}(\text{NO}_3)_2 \cdot 4\text{H}_2\text{O}$ ), 8-hydroxyquinoline ( $\text{C}_9\text{H}_7\text{NO}$ ), acetic acid ( $\text{CH}_3\text{COOH}$ ) and ammonium solution ( $\text{NH}_4\text{OH}$ ), all of analytical purity were used as starting materials. The calcium nitrate and 8-hydroxyquinoline were combined to yield a composition with the general formula  $\text{Ca}(\text{C}_9\text{H}_7\text{NO})_2$ . The ratio of nitrate to quinoline used was 1:2. Ammonium hydroxide ( $\text{NH}_4\text{OH}$ ) and acetic acid were used respectively as precipitating and acidic agents. 8-hydroxyquinoline ( $\text{C}_9\text{H}_7\text{NO}$ ) was slowly dissolved in 25 ml double distilled water and then 10 ml of acidic acid was added into the solution. The solution was then stirred well at  $50^\circ\text{C}$  for 4 hr. An orange transparent solution was obtained. This was referred to as mixture-1. In a separate glass beaker, calcium nitrate was dissolved in 15 ml double distilled water, was stirred vigorously at  $50^\circ\text{C}$  for 1 hr and resulted in a transparent solution that was referred to as mixture-2. The two mixtures were combined and the resulting suspension was stirred at  $50^\circ\text{C}$  for 1 hr. A solution of  $\text{NH}_4\text{OH}$  (precipitating agent) was then added drop by drop while stirring continuously until a yellowish green precipitated was formed. The precipitate was filtered out, and was washed several times with double distilled water to remove unwanted unreacted impurities. The sample was then kept at  $80^\circ\text{C}$  to dry. The three steps reaction mechanism for the formation of the  $\text{Caq}_2$  is presented in Fig. 1.

**Fig. 1** The overview synthesis mechanism of  $\text{Caq}_2$  powder sample



## Thin Film Preparation

PMMA blended  $\text{Caq}_2$  thin film was prepared by mixing solutions of 1 g of PMMA and 0.1 g of  $\text{Caq}_2$  respectively in 20 and 10 ml of chloroform. The mixture was stirred vigorously and the resulting solution was transferred to a stainless steel plate and was dried at room temperature. The molar concentration ratio of  $\text{Caq}_2$  to PMMA in the film was 0.1:1.

## Characterization Techniques

The powder and thin films were characterized by X-ray diffraction using a Bruker XRD with  $\text{CuK}\alpha$  radiation ( $\lambda=1.541 \text{ \AA}$ ). The morphology of the  $\text{Caq}_2$  powder analyses was carried out using a Shimadzu's SSX-550 scanning electron microscope (SEM). Atomic Force Microscopy (AFM) pictures were obtained from the Shimadzu SPM-9600 model. TG–DTA data were collected using a Perkin-Elmer Pyris Diamond TG–DTA instrument at a heating rate of  $10 \text{ }^\circ\text{C}/\text{min}$  under a dry air atmosphere using  $\alpha$ -alumina ( $\text{a-Al}_2\text{O}_3$ ) as a standard. An infrared spectrum of the sample was recorded using a Perkin-Elmer Spectrum One FT-IR spectrophotometer using the KBr disk method. Perkin Elmer LS950 lambda UV–Vis spectrophotometer was used to study absorption bands of the  $\text{Caq}_2$  powder. The photoluminescence (PL) properties of the  $\text{Caq}_2$  powder and blended  $\text{Caq}_2$ -PMMA thin films were measured using a Shimadzu spectrophotometer (RFPC-5301) at room temperature using a monochromatized Xenon flash lamp as an excited source. The chemical composition of the  $\text{Caq}_2$  powder was analyzed using a PHI 5000 *versa probe* X-ray photoelectron spectrometer (XPS). The XPS data were collected when the samples were irradiated with a monochromatic  $\text{Al K}\alpha$  radiation ( $h\nu=1486.6 \text{ eV}$ ). Survey scans were recorded using a  $1 \text{ eV}/\text{step}$  (binding energies ranging from 0 to 1400 eV). The sample area analyzed was about  $1 \text{ mm}^2$  and the pressure during data acquisition was typically under  $1 \times 10^{-8} \text{ Torr}$ . The experimental curves were fitted using a *multipack v8.2c* data analysis software provided with the PHI-5000 *versa-probe* ESCA instrument that made use of a combination of Gaussian–Lorentzian lines.

## Results and Discussion

### Structure and Morphology Analysis

The XRD patterns of  $\text{Caq}_2$  powder and  $\text{Caq}_2$ :PMMA are shown in Fig. 2. The sharp diffraction peaks that were indexed to the crystalline structure of  $\text{Caq}_2$  were detected from the powder sample. In the case of the blended  $\text{Caq}_2$ :PMMA thin film, a limited number of diffraction peaks produce from the amorphous background suggesting that the film was a mixture of crystalline and amorphous phases.

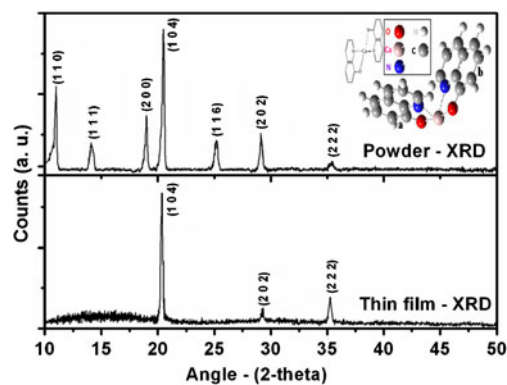


**Fig. 2** XRD pattern of the  $\text{Caq}_2$  powder and thin film of  $\text{Caq}_2$ :PMMA (0.1:1ratio), (inset the molecular structure of the  $\text{Caq}_2$  matrix)

The measured peak positions and relative intensities are listed in Table 1. The difference in the diffraction pattern of the powder and thin film suggests that the crystalline phase of the  $\text{Caq}_2$  powder in the resulting film has changed [11], which may be due to the interactions between the  $\text{Caq}_2$  molecule and the oxygen atoms in the PMMA chains. Although the structure of  $\text{Caq}_2$  has not been reported yet, we speculate that it crystallized in a stable tetramic phase, i.e.  $(\text{Caq}_2)_4$ . This speculation is consistent with the structure of  $\text{Znq}_2$  whose chemical formula is in many respects similar to that of  $\text{Caq}_2$ . Note that the crystal structures of both dihydrate and anhydrous  $\text{Znq}_2$  have been predicted by theoretical studies. The dihydrate  $\text{Znq}_2$  is predicted to crystallize in planer geometries while the studies of anhydrous  $\text{Znq}_2$  predicted distorted planar or tetrahedral geometries [7, 12]. A few reports based on theory and experiments suggest that anhydrous  $\text{Znq}_2$  (in powder or thin film form) have a tetrameric structure  $(\text{Znq}_2)_4$  with two  $\text{Zn}^{2+}$  ion centres with six- and five-coordinate geometry [12, 13]. In addition, Hopikins et al. [8] suggest that  $\text{Znq}_2$  may exist as tetramers in chloroform solvent but partially dissociate to

**Table 1** Measured XRD peak positions and relative intensities of powder ( $\text{Caq}_2$ ) and thin film ( $\text{Caq}_2$ :PMMA)

	Peak position ( $2\theta$ )	Relative Intensity (a. u.)
Powder	10.98	379
	14.12	135
	19.06	205
	20.59	614
	25.18	145
	29.10	174
	35.40	50
Thin film	20.23	582
	29.25	76
	35.24	130

monomers in nucleophilic solvent such as DMSO (Dimethyl sulfoxide). Similarly, we propose a stable tetrameric  $[(Caq_2)_4]$  with two distinct crystallographic Ca  $[Ca_1$  and  $Ca_2]$  atoms of different coordination geometries. Consistent with the Zn atoms in the  $(Znq_2)_2$  structures discussed in ref. [7],  $Ca_1$  are penta-coordinated while  $Ca_2$  atoms are hexa-coordinated resulting in a distorted octahedral geometry. The structural overview of the  $Caq_2$  in the inset of Fig. 2 was drawn according to similar zinc quinolate  $(Znq_2)$  structure reported in ref [7]. According to this structure,  $Caq_2$  metal chelates composed of one metal calcium ion ( $Ca^{2+}$ ) and two 8-hydroxyquinoline molecules. Figure 3 (a) and (b) show the low and high magnification SEM images of the  $Caq_2$  powder while figures (c) and (d) show the two and three dimensional AFM images of the  $Caq_2$ :PMMA thin film. The  $Caq_2$  powder consisted mainly of porous and spheroidal chunks of particles whose diameter is in the range of 10–20  $\mu m$ . The enlarged SEM image in Fig. 3(b) suggests that the chunks of powder were formed from an agglomeration of a large number of smaller particles. The  $Caq_2$  powder is distributed evenly along the PMMA polymer film as clearly observed from the 2-d and 3-d images of the AFM pictures shown in Fig. 3(c) and (d).

### Thermogravimetric Analysis of Powder Sample

The TG–DTA curves of the  $Caq_2$  powder are shown in Fig. 4. The endothermic peaks due to the melting and vaporization of water and 8-Hq (8-hydroxyquinoline) at around 122.5 and 326.7  $^{\circ}C$  were absent in the DTA curves, suggesting that there were no phases of unreacted 8Hq in the final product [14]. The endothermic reaction of the  $Caq_2$  starting from room temperature, which was accompanied by a weight loss, is ascribed to desorption of adsorbed moisture. Note that  $Caq_2$  was prepared at a temperature of 80  $^{\circ}C$  under ambient conditions, and therefore a very small amount of adsorbed  $H_2O$  was probably present on the surface. The TGA analysis (Heat flow) of  $Caq_2$  showed that the gas evolved at 122.5  $^{\circ}C$  was in the form of water vapour [14]. In the TGA curves of the  $Caq_2$  the second weight loss, which was only a very small percentage (less than 2 %) was observed in the 140–326.7  $^{\circ}C$  temperature range. In the corresponding DTA curve of the  $Caq_2$  the exothermic peak, which was observed at the 120–240.4  $^{\circ}C$  temperature range, can be ascribe to the dehydration of the coordinated water molecules ( $H_2O$ ) of the intercalated complex [13]. The DTA curve followed the partial decomposition of the anhydrous complex [15] near 337.9  $^{\circ}C$ . In the corresponding DTA

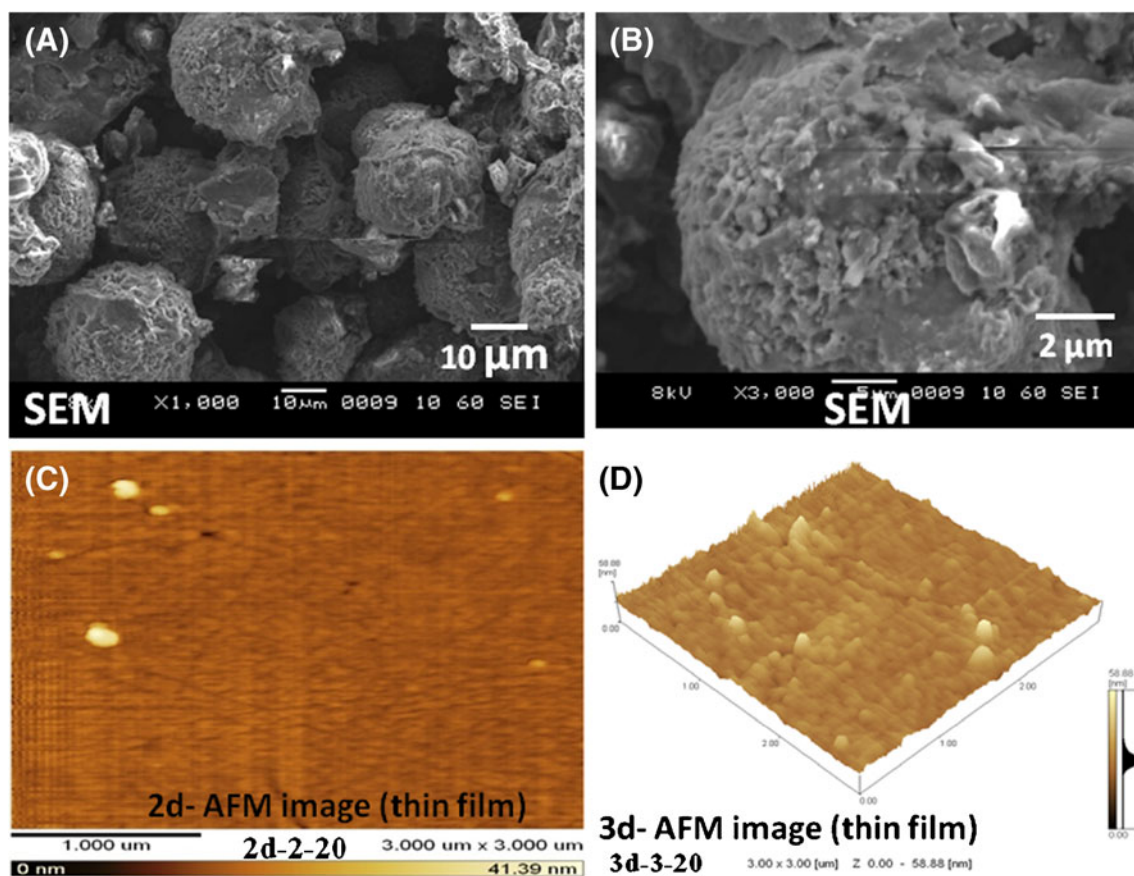
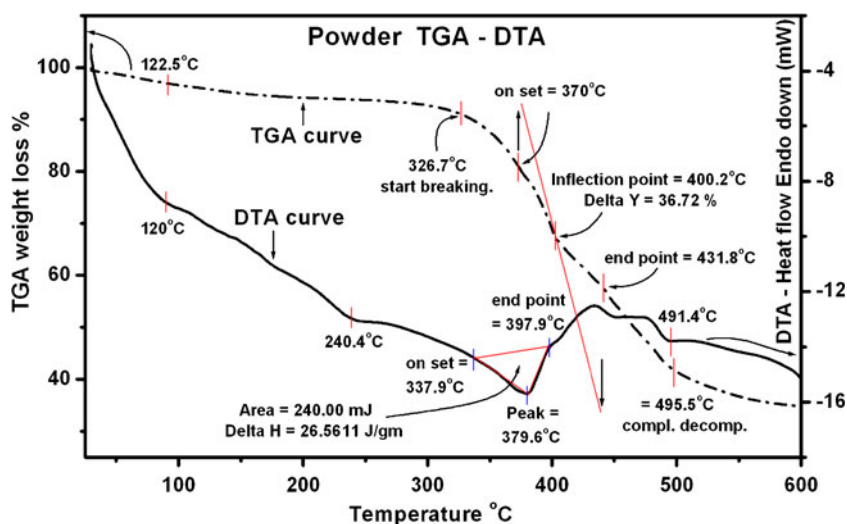


**Fig. 3** a, b, c and d SEM micrographs of  $Caq_2$  powder and AFM micrograph of the thin film of  $Caq_2$ :PMMA

**Fig. 4** TG-DTA spectrum of the Caq<sub>2</sub> powder



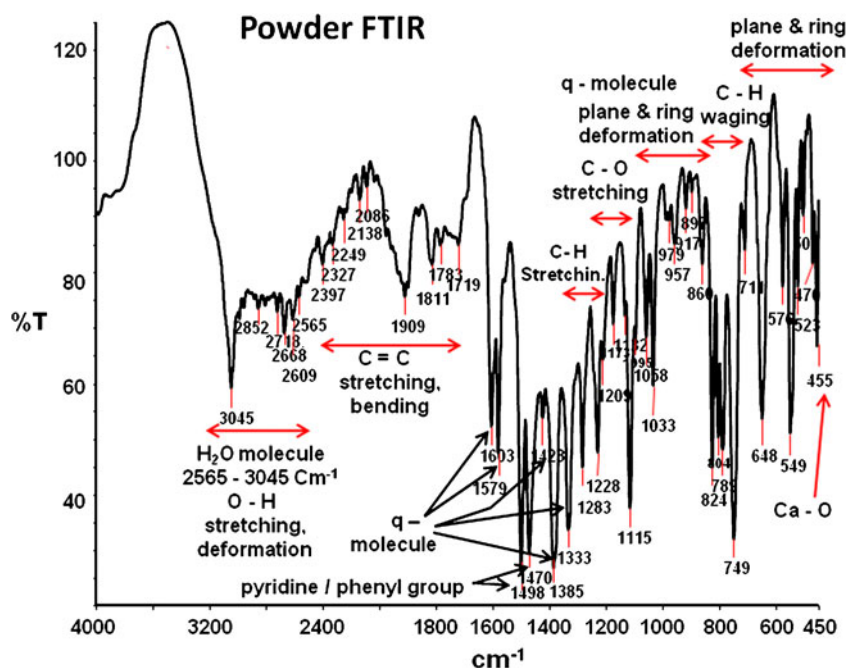
curve, the exothermic peak was observed at 379.6 °C and is ascribed to the volatilization and/or the decomposition of the anhydrous Caq<sub>2</sub> complex, which is in consistent with zinc quinolate [14]. The third weight loss between 370 and 431.8 °C from the TGA curve corresponds to the exothermic peak at 379.6 °C in the DTA curve. In the DTA curve, the peak at 397.9 °C can be attributed to the evaporation and oxidative decomposition of the coordinated 8Hq, which is consistent with other metal (Zn, Nb, Pb) quinolates [16]. The last weight loss between 431.8 and 495.5 °C in the TGA curve occurred concurrently with the exothermic peaks between 397.9 and 491.4 °C in the DTA curve. The last weight loss occurring between 431.8 and 495.5 °C can be attributed to the final pyrolysis of 8Hq [17]. By comparing the TG–DTA curves of

the host materials, the thermal behavior was ascribed to the decomposition of intercalated 8Hq from Caq<sub>2</sub> phosphor.

FTIR Spectroscopic Analysis of Powder Sample

In the FTIR spectra of the Caq<sub>2</sub> powder shown in Fig. 5, the absorption bands are characteristic of the 8Hq. The C–H out of plane bending and wagging modes with strong relative intensities were detected at 711, 749, and 804 cm<sup>-1</sup> and the plane stretching modes were detected at 1209, 1228 and 1283 cm<sup>-1</sup> [18]. The absorption bands in the range of 1719–2397 cm<sup>-1</sup> were characteristics of 8Hq that can be assigned to the C=C plane bending and stretching modes. These bands were slightly shifted to higher frequency

**Fig. 5** FTIR spectrum of the Caq<sub>2</sub> powder



regions compared to free 8Hq molecules [18]. This is due to the coordination between the 8Hq molecule and the calcium exchanged cation in the interlayer spaces of  $\text{Caq}_2$ . This confirms the chelation between 8Hq and metal cations Ca (II) in the interlayer spaces of  $\text{Caq}_2$ . The characteristic absorption bands ascribed to  $\text{Caq}_2$  were observed at 648, 576, 549, 523 and  $470\text{ cm}^{-1}$  and can be ascribed to the plane and ring deformation of the intercalated complex. These data are in agreement with the FTIR data of  $\text{Znq}_2$  reported in ref [19]. The plane and ring deformation of 8Hq peaks were observed at around  $860\text{--}979\text{ cm}^{-1}$ . The absorption characteristics band of Ca-O was observed at  $455\text{ cm}^{-1}$  [20]. The metal bonding with the quinoline molecules are given by the characteristics peaks at 1333, 1385, 1423, 1579 and  $1603\text{ cm}^{-1}$  [19]. The phenyl/pyridine hydroxyl group of 8-hydroxyquinoline ring shows two characteristic peaks at 1470 and  $1498\text{ cm}^{-1}$  due to the phenyl groups [21]. The O-H vibration bands were detected at  $2565\text{--}3045\text{ cm}^{-1}$  [21]. The wave numbers ( $\text{cm}^{-1}$ ) of infrared bands of the products and their assignments are listed in Table 2. The FTIR spectra did not show any additional absorption bands due to decomposed species, confirming no decomposition of 8Hq. This strongly suggests that stable  $\text{Caq}_2$  complex was formed.

## Absorption and PL Analyses

### Absorption Measurement

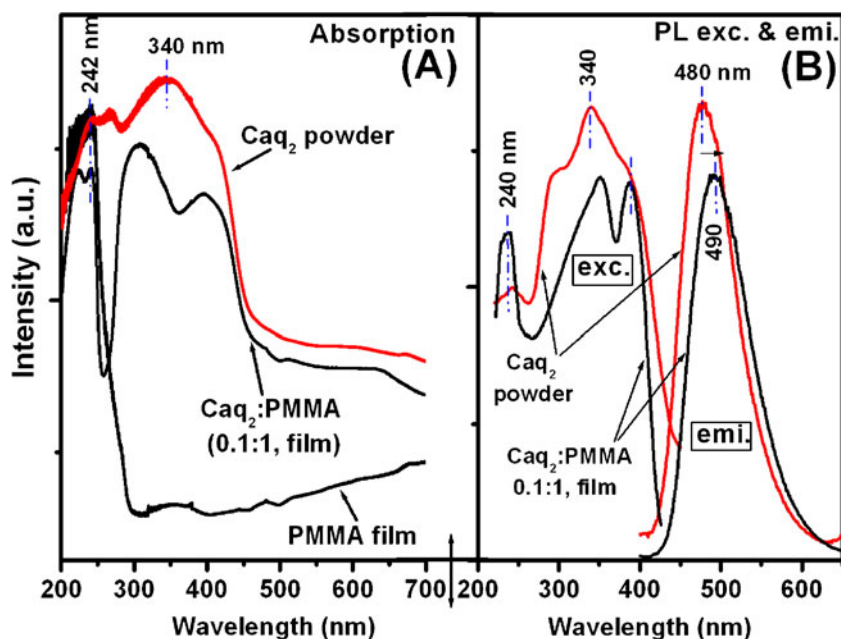
The diffuse absorption spectra of  $\text{Caq}_2$  powder,  $\text{Caq}_2$ :PMMA (0.1:1) thin film and pure PMMA film are shown in Fig. 6(a). The major absorption band of the  $\text{Caq}_2$  powder was observed at around 340 nm with a shoulder at 410 nm. The band at 340 nm is assigned to electron

**Table 2** Wavenumbers ( $\text{cm}^{-1}$ ) of infrared bands of the products and their assignments

Assignments	$\text{Caq}_2$
Ca-O	455
Ring deformation	470, 460, 523, 549, 576
q-molecule stretching, ring deformation	860, 897, 917, 979, 1033, 1058
C-H wagging	648, 711, 74, 9781, 804
C-O stretching	1095, 1100, 1115
C-H stretching	1209, 1228, 1283
q-molecule	1333, 1385, 1423, 1579, 1603
Phenyl /pyridine	1470, 1498
C=C stretching, bending	1719–2397
O-H vibration, stretching, bending of $\text{H}_2\text{O}$	2565–3045

transition from the HOMO orbit in the phenoxide ring to the LUMO orbit in the pyridine ring due to  $\pi\text{--}\pi^*$  bonding of the 8-hydroxyquinoline unit of the calcium complex. The absorption band that was observed at around 260 nm can be ascribed to a charge transfer state of the calcium metal ion to the 8Hq molecule. These ascriptions are consistent with the  $\text{Znq}_2$  absorption reported in ref [22]. The absorption spectra of  $\text{Caq}_2$ :PMMA thin film gave some major bands at 320 and 410 nm. Note that the  $\sim 240\text{ nm}$  bands is more pronounced in the film compared to the powder sample, which was in turn prominent in pure PMMA film and it can therefore be assigned to PMMA [23]. This splitting and shifting of absorptions were probably a result of different orientations of the metal quinolate molecules in  $\text{Caq}_2$  powder versus  $\text{Caq}_2$ :PMMA blended thin film is similar to earlier reports [24].

**Fig. 6** a Absorption spectrum and b PL spectrum of the  $\text{Caq}_2$  powder and thin film of  $\text{Caq}_2$ :PMMA



These differences were also clearly observed in the XRD patterns in Fig. 2. Another possibility in splitting of the absorption bands might be changes in the band gap between HOMO and LUMO following the reaction between the oxygen in the PMMA with the 8Hq molecule. This behavior was also observed in the photoluminescence excitation spectra shown in Fig. 6(b).

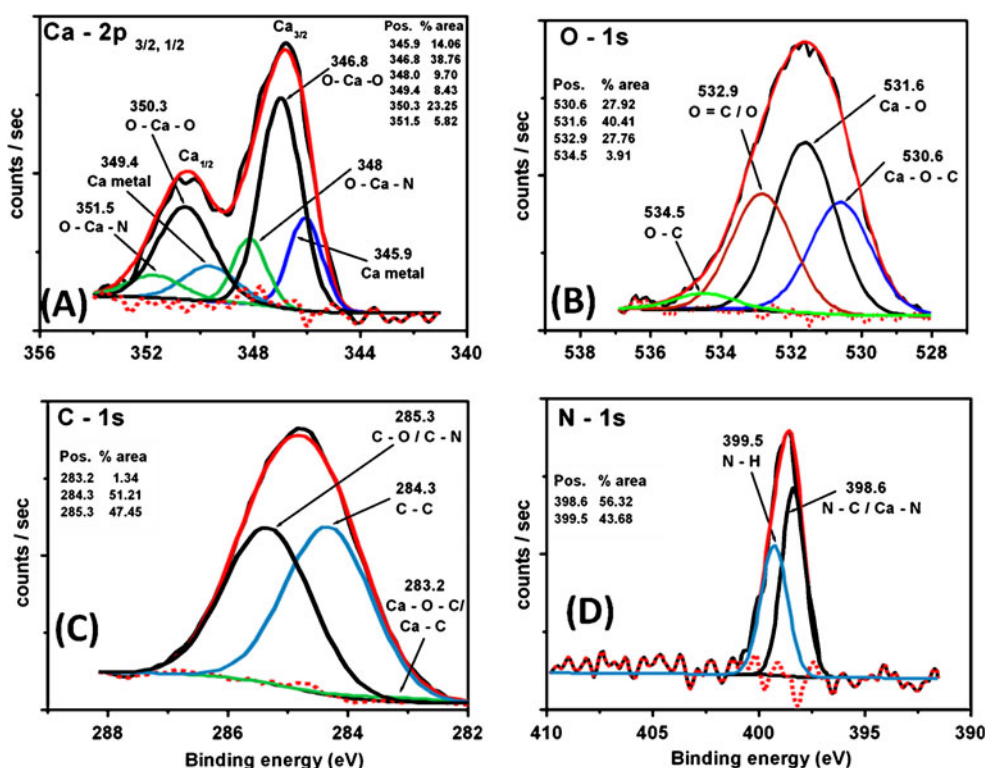
*Photoluminescence Measurement*

The photoluminescence (PL) excitation spectra of the Caq<sub>2</sub> powder and Caq<sub>2</sub>:PMMA thin film in Fig. 6 (b) compares very well with the data in Fig. 6(a). The PL emission spectra monitored when the samples were excited at 340 nm for the powder Caq<sub>2</sub> and thin film are also shown in Fig. 6(b). The spectra show bluish-green photoluminescence at 480 and 490 nm from the powder and thin film respectively. These emissions can be assigned to  $\pi-\pi^*$  transition localized on the quinoline rings [25]. The PL emission of the Caq<sub>2</sub>:PMMA (0.1:1) film was red shifted by 10 nm from the PL emission of the powder. The red-shift in the PL emission of the film suggested that there is significant delocalization of  $\pi-\pi^*$  transition [26] of the excited state along the PMMA polymer chains. The extended delocalization in the film may occur due to the PMMA groups, which attached at the 5-position of the quinolate ligand [27].

XPS Analysis of Caq<sub>2</sub> Powder

The high resolution XPS peaks of Ca-2p, O-1 s, C-1 s and N-1 s were deconvoluted using the *MultiPak*<sup>TM</sup> [28] software program. Figure 7(a) shows the high resolution XPS scan of the Ca-2p of the powder sample. The Ca-2p is deconvoluted into six peaks with binding energy (B.E.) values at 345.9, 346.8, 348, 349.4, 350.3 and 351.5 eV. These six peaks can be ascribed to the components of the split 2p<sub>3/2</sub> and 2p<sub>1/2</sub> energy states. The peaks at 345.9 (2p<sub>3/2</sub>) and 349.4 (2p<sub>1/2</sub>) eV are probably coming from pure Ca-Ca bonding [29]. The peak at 346.8 (2p<sub>3/2</sub>) and 350.3 (2p<sub>1/2</sub>) eV corresponds to calcium bonded to oxygen in the O-Ca-O bonding series [30]. The peak at 348 (2p<sub>3/2</sub>) and 351.5 (2p<sub>1/2</sub>) eV can be assigned to the O-Ca-N chemically bonding [30]. The deconvoluted oxygen O-1 s XPS high resolution peak is shown in Fig. 7(b). The O-1 s XPS scan was deconvoluted into four peaks at 530.6, 531.6, 532.9 and 534.5 eV. The binding energy (B.E.) values of O-1 s at 530.6 eV, 531.6 eV and 532.9 can be respectively be assigned to Ca-O-C to Ca-O and O=C/O bonding [31]. The B.E. value of O-1 s centered at 534.5 eV corresponds to the O-C bonding [31]. The B.E. value with small shoulder centred at 536.5 eV in the complex is probably due to adsorbed moisture associated with hygroscopic hydroxide species, i.e. the C/H-OH bonding [32]. These additional species indicate the presence of small amount of water in the Caq<sub>2</sub> matrix which was also confirmed by FTIR data in Fig. 5. The carbon

**Fig. 7** a, b, c, d High resolution XPS spectra and deconvolution of the a Ca-2p, b O-1 s, c C-1 s and d N-1 s signal for the Caq<sub>2</sub> powder phosphor



C-1 s scan of the Caq<sub>2</sub> powder sample was deconvoluted into three peaks centered at 283.2, 284.3 and 285.3 as shown in Fig. 7(c). The binding energy (B.E.) values of C-1 s at 283.2, 284.3 and 285.3 eV can respectively be assigned to Ca-O-C/Ca-C C-C and C-O/C-N bonding [32]. The XPS peaks of N-1 s are shown in Fig. 7(d) and are split into two components with BE values of 398.6 and 399.5 eV, which which can be assigned to N-C and N-H bonding [30] respectively. The XPS binding energy values of deconvoluted Ca-2p, O-1 s, C-1 s and N-1 s XPS peaks confirming the bonding between Ca-Ca, O-Ca-O, O-Ca-N, Ca-O-C/Ca-C, C-C/C=C, N-C, N-H and O=C/O clearly suggests the successful formation of the Caq<sub>2</sub> complex.

In summary, XRD confirm the formation of Caq<sub>2</sub> powder, while the thin film of Caq<sub>2</sub>:PMMA contains the major peaks and re-orientation of molecular structure of Caq<sub>2</sub> occurred. The bluish-green emission was observed in the powder sample, while a 10 nm red-shifted photoluminescence in the thin film was observed. The DG-DTA confirms the thermal stability up to  $\approx 380$  °C of the powder sample. The FTIR and XPS analysis confirm the formation of the Caq<sub>2</sub> complex. The broad band excitation in the range of 300–420 nm confirms that the powder and film might be useful in the OLED applications.

## Conclusion

Caq<sub>2</sub> (calcium 8-hydroxyquinoline) organic phosphor was synthesized by a low cost and conventional co-precipitation method. The XRD and FTIR confirmed the formation of the Caq<sub>2</sub> compound and the XPS analysis confirms the chemical bonding between the elements. The SEM image showed that chunk of spheroidal particles were an agglomeration of smaller particles and the AFM images suggest the continuous distribution of particles in the PMMA matrix. The DG-DTA analysis of the powder sample suggests that Caq<sub>2</sub> is thermally stable up to 380 °C. The optical properties such as absorption and PL were evaluated and compared for the Caq<sub>2</sub> powder and thin film of Caq<sub>2</sub>:PMMA (0.1:1) Caq<sub>2</sub> compound. The bluish-green PL emission was observed at 480 nm and 490 nm from the powder and the film respectively. The red shift of 10 nm in the film compared to powder sample was ascribed to re-orientation and significant delocalization  $\pi-\pi^*$  transition of the Caq<sub>2</sub> molecular structure when the powder was mixed with the PMMA solution. The observed optical properties of the Caq<sub>2</sub> powder and thin film suggest that this compound is a potential candidate for application in organic light emitting devices such as OLEDs.

**Acknowledgement** Authors are thankful to the University of the Free State (UFS) cluster program and the South African National Research Foundation (NRF) for the financial support.

## References

1. Vivas-Reyes R, Nunez-Zarur F, Martinez E (2008) Electronic structure and reactivity analysis for a set of Zn-chelates with substituted 8-hydroxyquinoline ligands and their application in OLED. *Org Electro* 9:625–634
2. Manju R, Blanton Thomas N, Tang Ching W, Lenhart William C, Switalski Steven C, Giesen David J, Antalek Brian J, Pawlik Thomas D, Kondakov Denis Y, Nicholas Z, Young Ralph H (2009) Structural, thermal, and spectral characterization of the different crystalline forms of Alq<sub>3</sub>, tris(quinolin-8-olato) aluminum(III), an electroluminescent material in OLED technology. *Polyhedron* 28:835–843
3. Mei Q, Du N, Lu M (2006) Synthesis and characterization of high molecular weight metaloquinolate containing polymers. *J Appl Poly Sci* 99:1945–1952
4. Du N, Tian R, Peng J, Lu M (2005) Synthesis and photo-physical characterization of the free-radical copolymerization of metaloquinolate-pendant monomers with methyl methacrylate. *J Poly Sci: Part A: Poly Chem* 43:397–406
5. Stefan B, Wolfgang B (2002) Dispersive electron transport in tris (8-Hydroxyquinoline) aluminum (Alq<sub>3</sub>) probed by impedance spectroscopy. *Phys Rev Lett* 89:286601
6. Duvenhage MM, Ntwaeborwa OM, Swart HC (2012) UV exposure and photon degradation of Alq<sub>3</sub> powders. *Physica B: Phys of Conden Matt* 407(10):1521–1524
7. Sapochak LS, Benincasa FE, Schofield RS, Baker JL, Riccio KKC, Fogarty D, Kohlmann H, Ferris KF, Burrows PE (2002) Electroluminescent zinc(II) bis(8-hydroxyquinoline): Structural effects on electronic states and device performance. *J Am Chem Soc* 124:6119–6125
8. Hopkins TA, Meerholz K, Shaheen S, Anderson ML, Schmidt A, Kippelen B, Padias AB, Hall JHK, Peyghambarian N, Armstrong NR (1996) Substituted aluminum and zinc quinolate with blue-shifted absorbance/luminescence bands: synthesis and spectroscopic, photoluminescence, and electroluminescence characterization. *Chem Mater* 8:344–351
9. European Patent Specification, Bulletin 2004/12 EP 1144543 B1
10. Cheng CH, Jianmin S (1998) Metal chelates as emitting materials for organic electroluminescence. *Coord Chem Rev* 171:161–174
11. El-Nahass MM, Farid AM, Atta AA (2010) Structural and optical properties of Tris(8-hydroxyquinoline) aluminum (III) (Alq<sub>3</sub>) thermal evaporated thin films. *J Alloys and Compds* 507:112–119
12. Bing-she Xu, Hao Yu-ying, Wang H, Zhou He-feng, Liu Xu-guang, Chen Ming-wei (2005) The effects of crystal structure on optical absorption/ photoluminescence of bis (8-hydroxyquinoline) zinc. *Solid State Commun* 136:318–322
13. Kai Y, Moraita M, Yasuka N, Kasai N (1985) The crystal and molecular structure of anhydrous zinc 8-quinolinolate complex, (Zn(C<sub>9</sub>H<sub>6</sub>NO)<sub>2</sub>)<sub>4</sub>. *Bull Chem Soc Jpn* 58:1631–1635
14. Nithima K, Makoto O (2010) Formation of mono(8-hydroxyquinoline) lithium(I) complex in smectites by solid–solid reactions. *J Phys and Chem Solids* 71:1644–1650
15. Crespi MS, Ribeiro CA, Greenhalf VCM, Zorel HE Jr (1999) Preparation and thermal decomposition of copper(II), zinc(II) and cadmium(II) chelates with 8-hydroxy quinoline. *Quimica Nova* 22:41–46
16. Juiz SA, Leles MIG, Caires ACF, Boralle N, Ionashiro M (1997) Thermal decomposition of the magnesium, zinc, lead and niobium chelates derived from 8-Quinolinol. *J Therm Anal* 50:625–632
17. Pastre IA, Oliveria IDN, Moitinho ABS, de Souza GR, Ionashiro EY, Fertonani FL (2004) Thermal behaviour of intercalated 8-hydroxyquinoline (oxine) in montmorillonite clay. *J Therm Anal Calorim* 75:661–669

18. Marchon B, Bokobza L, Cote G (1986) Vibrational study of 8-quinolinol and 7-(4-ethyl-1-methyloctyl)-8-quinolinol (Kelex 100), two representative members of an important chelating agent family. *Spectrochim Acta* 42A:537–542
19. Magee RJ, Gordon L (1963) The infrared spectra of chelate compounds-I: a study of some metal chelate compounds of 8-hydroxyquinoline in the region 625 to 5000  $\text{cm}^{-1}$ . *Talanta* 10:851–859
20. Atalay S, Adiguzel HI, Atalay F (2001) Infrared absorption study of  $\text{Fe}_2\text{O}_3\text{-CaO-SiO}_2$  glass ceramics. *Mater Sci and Eng A* 304:796–799
21. Tackett JE, Sawyer DT (1964) Properties and infrared spectra in the potassium bromide region of 8-quinolinol and its metal chelates. *Inorg Chem* 3:692–696
22. Bingshe X, Hua W, Yuying H, Zhixiang G, Hefeng Z (2007) Preparation and performance of a new type of blue light-emitting material  $\delta\text{-Alq}_3$ . *J Lumin* 122:663–666
23. Ayako T, Hirose H (1998) Wavelength effect on the accelerated photo-degradation of polymethylmethacrylate. *Poly Degrad and Stab* 61:361–364
24. Garbuzov DZ, Bulovi V, Burrows PE, Forrest SR (1996) Photoluminescence efficiency and absorption of aluminum-tris-quinolate ( $\text{Alq}_3$ ) thin films. *Chem Phys Lett* 249:433–437
25. Zhong Chaofan Wu, Qian GR, Hailiang Z (2008) Synthesis and luminescence properties of polymeric complexes of Cu(II), Zn(II) and Al(III) with functionalized polybenzimidazole containing 8-hydroxyquinoline side group. *Opt Mater* 30:870–875
26. Wang X-Y, Weck M (2005) Poly(styrene)-supported  $\text{Alq}_3$  and  $\text{BPh}_2\text{q}$ . *Macromolecules* 38:7219–7224
27. Mahakhode JG, Bahirwar BM, Dhoble SJ, Moharil SV (2006) Tunable Photoluminescence from tris(8-Hydroxyquinoline) Aluminum ( $\text{Alq}_3$ ). *Proc of ASID, New Delhi* 237–239
28. MultiPak<sup>TM</sup> Version 9 (2006–2010) Physical Electronics, Inc. Chanhassen, USA
29. Selvam P, Viswanathan B, Srinivasan V (1989) XPS studies of the surface properties of  $\text{CaNi}_5$ . *J Electron Spectrosc Relat Phenom* 49 (2):203–211
30. Demri B, Muster D (1995) XPS study of some calcium compounds. *J Mater Proces Techno* 55:311–314
31. Voigts F, Bebensee F, Dahle S, Volgmann K, Maus-Friedrichs W (2009) The adsorption of  $\text{CO}_2$  and CO on Ca and CaO films studied with MIES, UPS and XPS. *Surf Sci* 603:40–49
32. Jean-Charles D, Danielle G, Philippe V, Alain L (2000) Systematic XPS studies of metal oxides, hydroxides and peroxides. *Phys Chem Chem Phys* 2:1319–1324